Experimental investigation of the sliding failure mode in full-scale squat reinforced concrete shear wall specimen

Author(s):
Pizarro Pohl, Diego; Kovarbasic, Milan; Stojadinovic, Bozidar

Publication date:
2022

Permanent link:
https://doi.org/10.3929/ethz-b-000584291

Funding acknowledgement:
184805 - Quasi-Dynamic Seismic Performance-Based Design Procedure (SNF)

3rd EUROPEAN CONFERENCE ON
EARTHQUAKE ENGINEERING & SEISMOLOGY
BUCHAREST, ROMANIA, 2022

Experimental investigation of the sliding failure mode in full-scale squat reinforced concrete shear wall specimen

Diego Pizarro – ETH Zürich, Zürich, Switzerland, e-mail: pizarro@ibk.baug.ethz.ch

Milan Kovarbasic – ETH Zürich, Zürich, Switzerland, e-mail: kovarbasic@ibk.baug.ethz.ch

Bozidar Stojadinovic – ETH Zürich, Zürich, Switzerland, e-mail: stojadinovic@ibk.baug.ethz.ch

Abstract: Squat-reinforced concrete shear walls are used as a gravity and lateral load resisting system in structures such as buildings and nuclear power plants. Due to their low aspect ratio, they are prone to shear or sliding failure. A shear wall was subjected to a cyclic test at the new Multi-Axis Sub-Assemblage Testing (MAST) facility at ETH Zurich. The shear to span ratio was 0.51 and a vertical load of 5.61% of the axial capacity of the wall was applied. The wall had a sliding failure, with a peak load capacity of 2760 kN. Digital Image Correlations (DIC) results show how the shear crack developed until sliding started and, from this point on, the majority of the wall deformation originated in the wall-foundation interface. Sliding displacements consisted of more than 50% of the total displacements of the specimen in large-amplitude cycles.

Keywords: Shear wall, sliding, reinforced concrete, test, failure mode

1. Introduction

Reinforced concrete shear walls are structural elements commonly used for gravity and lateral load resistance systems. Their deformation could be decomposed into four response modes: flexure, shear, sliding, and rocking (associated with reinforcement bond-slip deformations). The deformation of a wall could be governed by one or a combination of them, or at large deformations, there could be a transition from one response mode to another, for instance, from flexure or shear to sliding.

Sliding failure consists of a relative displacement between two interfaces of a structural element. In a reinforced concrete wall, slip could occur in the cold joint between the wall and its foundation. This interface is formed after successive load cycles, in which cumulative residual tension strain in the reinforcement can open cracks along the wall length. With load reversal, the steel must yield in compression before the crack close, and if it does not, those cracks could remain open and generate a weak interface where sliding displacement can occur (Moehle 2015).

Sliding failure occurred in a fairly large number of shear wall tests. A database that reports tests with sliding failure can be found in Mangalathu et al (2020), and additional specimens not included in that database can be found in Luna et al (2013), Whyte and Stojadinovic (2014), Hube et al (2020), Baek et al (2020) and Terzioglu et al (2018). Furthermore, this failure was seen in a 4-story building tested at a shaking table test (Nagae et al 2015), where one shear wall had considerable sliding in the cold joint interface.

The mechanics of sliding and friction in reinforced concrete element interfaces have been widely studied. Walraven (1981), proposed relationships that described the aggregate interlock effect, which is the mechanism of transmission of forces across cracks whose faces are subjected to shear displacements. He proposed expressions, based on tests, which related

the stresses in the crack with the crack width and slip. These expressions have been further developed by Gambarova and Karakoç (1983) and Li (1989).

In shear walls, normal and shear stresses must be transferred and, due to bending, normal stresses are not constant and change along the length of the wall; this, in turn, means that shear stresses must be transferred through both tension and compression zones. Studies of transfer of shear stresses in tension have been conducted in concrete panels **by** Calvi et al (2017) and, on the other side, transfer in compression has been researched by Trost et al (2019). The latter proposed a mechanical model which considers bar kinging and aggregate interlock effect, with the addition of degradation of the aggregates.

3. ETHZ MAST Facility

The ETHZ MAST (Multi-Axis Sub-Assemblage Testing) Facility combines actuators, reaction walls, a crosshead, and a strong floor into an optimized machine that can handle a full node-wise coupling (3 translations and 3 rotations), between a numerical and physical sub-domain of a hybrid model (Abbiati and Stojadinovic 2018). It has 4 actuators in the Z direction (2 MN capacity each), 4 in X (1 MN each), and 2 in Y (1 MN each), and a crosshead of steel sections that transfers the loads from the actuators to the specimen (Figure 1).

The ETHZ MAST Facility can control the 6 degrees of freedom in force or displacement control, using a 12-channel digital controller developed by INOVA. This helps to control the boundary conditions and to apply axial force during a displacement or force control test.

To calibrate and test the facility, two pilot tests were conducted. The first specimen was a cylindrical steel column, and its main objective was to handle the six degrees of freedom control. In the second test, a squat reinforced concrete shear wall was subjected to cyclic loading to test the full-load capacity of the machine. The second test will be further described in this paper.

Fig. 1 – ETHZ MAST Facility

4. Shear wall specimen and its test

The specimen consists of a foundation, a wall, and a top cap-beam to facilitate the connection between the specimen and the ETHZ MAST cross-head. The geometry, material properties, and reinforcement are shown in Figure 2. The maximum concrete aggregate size is 16 mm.

Because the vertical reinforcement was continuous, the casting sequence was singular: the wall was cast horizontally (as a slab), then, it was stood up and the top beam was cast from the bottom. Then, the specimen was rotated and the foundation was cast from the bottom.

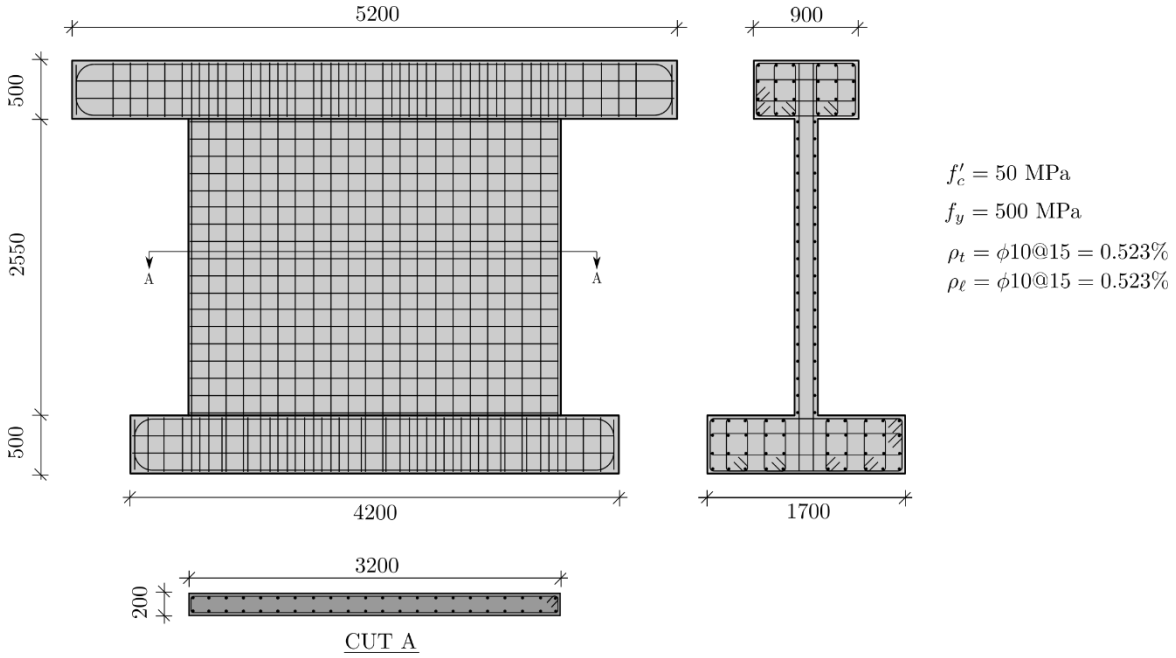

Fig. 2 – Specimen geometry and reinforcement. Non-displayed units in mm.

The specimen was fixed to the strong floor and the steel crosshead with steel rods post-tensioned to 1 MN (18 in the bottom and 12 in the top, Figure 1). As the test was conducted in-plane, torsion, and out-of-plane translation and rotation of the specimen were constrained. The control point of the test, where the displacements, rotations, forces, and moments are computed, was the center of the bottom flange of the steel crosshead, which is 3.25m above the interface wall foundation. The test was run in a fixed-fixed condition, which means that the system could not rotate at the control point, and therefore the shear-to-span ratio applied to the wall is M/VL = 0.51.

An axial load of 1.8 MN was applied, which corresponds to 5.63% of the axial capacity of the wall, and a series of increasing amplitude cycles were applied to the specimen (Table 1). As the specimen was quite stiff, the first two cycles were force-controlled (to 400 kN and 800 kN, respectively), whereas the subsequent cycles were in displacement control.

Each actuator has its load cell which measures its force. These values are then used by the MAST controller to compute forces and moments at the control point. Translations and rotations at the control point are calculated by using kinematic transformations with the measured elongations of each actuator. Several LDVTs were placed to measure sliding or rocking between different interfaces. One side of the specimen was speckled to measure strains with Digital Image Correlations system (DIC), while the other side was instrumented with an infra-red target system (NDI). No sensors were placed on the reinforcement bars.

5. Results

The control point horizontal force-displacement hysteresis curves are shown in Figure 3. Table 1 shows the displacement in each cycle, along with the proportion of the measured sliding deformation in the wall-foundation interface. The peak resistance was 2760 kN at a displacement of 20.81 mm (6.40‰ drift)

From cycle N°7 (11.93 mm), upon each load reversal, there is a plateau in which no increment of force is needed to deform the wall due to sliding. Sliding increased after each cycle, and in the last two cycles (N° 11 and 12) the hysteresis loop shape is very similar to a frictional damper. Previous sliding failures with no or low axial loads do not show this behavior: the axial load applied in this test engaged the friction at the wall-foundation interface to provide lateral load resistance.

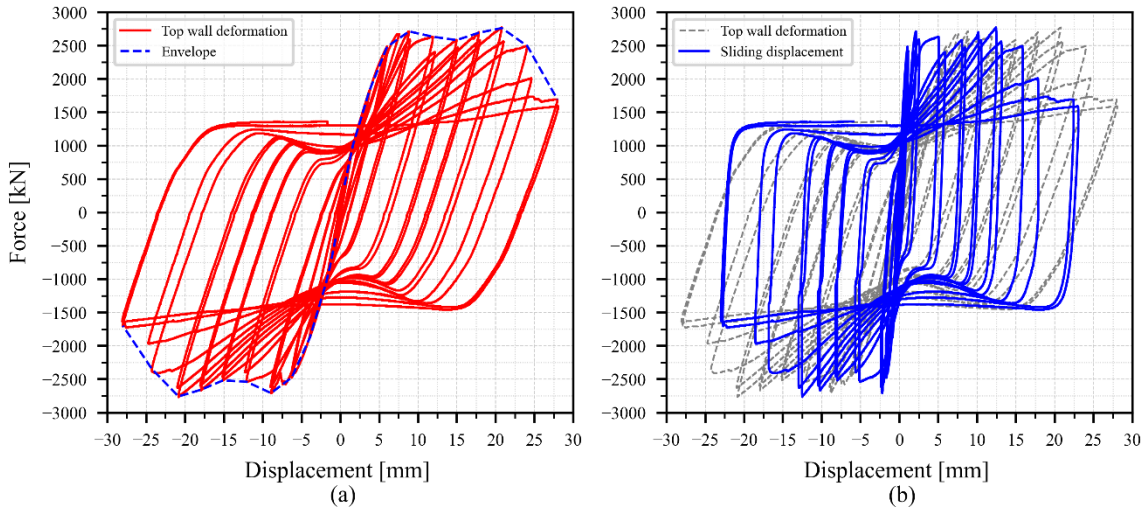

Figure 3: Control point horizontal force-displacement hysteretic curve: (a) total displacement; (b) sliding component of the total displacement.

Table 1. Measured specimen response. *Only positive cycles, as shown in Figure 3, are tabulated.*
** Cycles conducted in force control.*

Cycle	δ_{total} [mm]	Δ [‰]	First Cycle			Second Cycle		
			Force [kN]	$\delta_{sliding}$ [mm]	$\frac{\delta_{sliding}}{\delta_{total}}$ [%]	Force [kN]	$\delta_{sliding}$ [mm]	$\frac{\delta_{sliding}}{\delta_{total}}$ [%]
1*	0.55	0.17	400	0.06	11.56	400	0.06	11.50
2*	1.26	0.39	800	0.16	12.73	800	0.15	11.54
3	1.65	0.51	1011	0.21	12.91	1013	0.21	12.43
4	3.75	1.15	1821	0.58	15.49	1811	0.59	15.85
5	6.03	1.86	2479	1.04	17.31	2424	1.12	18.55
6	8.87	2.73	2710	2.13	23.98	2560	2.51	28.32
7	11.93	3.67	2630	4.97	41.65	2400	5.84	48.92
8	14.98	4.61	2580	7.99	53.33	2460	8.44	56.35
9	17.85	5.49	2690	10.17	56.98	2570	10.50	58.84
10	20.81	6.40	2760	12.43	59.76	2550	13.10	62.96
11	24.10	7.42	2490	15.73	65.26	1990	17.79	73.82
12	27.96	8.60	1690	18.87	67.50	1580	22.92	81.97

After the sliding failure was triggered, the sliding displacement increased in the second cycle at each displacement amplitude (Table 1). This is because of the degradation of the aggregate in the interface, and it is consistent with the effect and formulation described by Trost (2018).

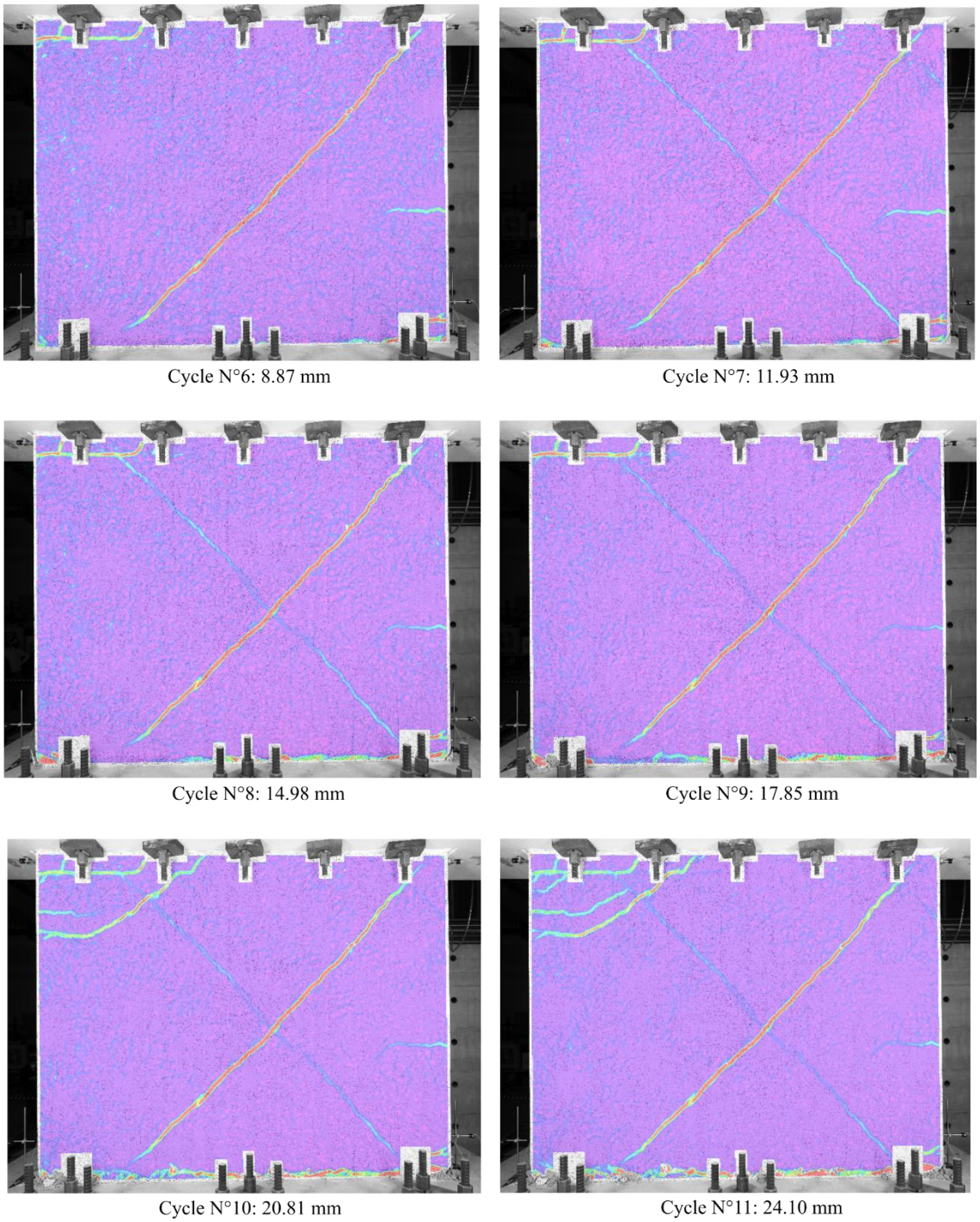

Figure 4: DIC displacement fields, showing the transition between shear and sliding.

An analysis of the displacement fields measures using DIC (Figure 4) shows the development of the transition between shear and sliding deformation. Up to a drift of 1.86‰ (Cycle N°5), one predominant diagonal shear crack was formed. But from this point on, that crack could not continue its development because most of the deformation was taking place due to sliding in the wall-foundation interface. This interface can be noted clearly in the DIC images from cycle N°8. Table 1 also shows that from cycles N° 6 to N° 7 there was a large increase in the contribution of sliding deformation, which indicates that the sliding failure started to take place in the sixth cycle.

Even though the wall reached a peak load larger than its sliding resistance, for large cycles the force was almost constant and equal to 1350 kN, 29% percent lower than the sliding strength of 1984 kN obtained with Equation 1 (ACI Committee 318, 2014):

$$V_{sliding} = \mu \cdot (A_s \cdot f_y + N) \qquad (1)$$

where μ is the friction coefficient (in this case, equal to 0.6), A_s the area of reinforcement perpendicular to the interface, f_y the yield strength of the steel, and N the axial load. This low sliding strength can be attributed to the casting procedure, as shown by Zhang et al (2020). In their experimental campaign in push-off tests, they reported a decrease in the bonding strength between two different layers of concrete as a consequence of casting from the bottom to the top.

6. Conclusions and future directions

A shear wall test was conducted at the ETHZ-MAST Facility. The wall reached a peak lateral load of 2760 kN and had a sliding failure.

To further investigate the transitions between different failure modes of squat shear walls, two experimental campaigns are currently being conducted, each one with a series of six specimens subjected to cyclic loading and hybrid simulation. The first one aims to study the transition between flexure and rocking, while the second targets to identify the transitions of shear/flexure to sliding. The specimens will be cast vertically to simulate on-site construction in both experimental campaigns.

In the experimental campaign related to the sliding transitions, the influence of different parameters will be investigated:

- Aspect ratio: Even though the aspect ratio does not directly affect the sliding resistance, it does to the flexure and shear strength.
- Reinforcement ratio: the steel reinforcement which crosses the sliding interface acts through its tension against the crack opening, preventing it to increase its width. On the contrary, reinforcement perpendicular to the sliding interface (usually horizontal) doesn't contribute directly to the sliding strength, but it affects the shear strength. Large reinforcement ratios mean larger shear strength, and therefore a sliding failure has a higher probability to occur.
- Axial load: the higher the axial load, the higher the sliding strength. This parameter is interesting to vary because the majority of the tests where sliding had occurred were conducted with zero or low levels of axial loads.
- Load sequence: As sliding failure develops throughout a displacement history, the type of load sequence will be investigated. For this purpose, two types of tests will be conducted: in-plane cyclic loading and hybrid simulation. Insights of this effect can be seen in tests conducted by Luna et al (2015) and Whyte and Stojadinovic (2014), where similar specimens were tested with different load sequences: the first one under cyclic tests, while the latter under hybrid simulation with a near-fault ground motion. In both cases, their specimens had a sliding failure.

Acknowledgements

This research is supported by the Swiss National Science Foundation (SNSF) under Grant 200021_184805 and the Swiss Federal Institute of Technology (ETH) Zurich. The authors gratefully acknowledge this funding. The methods, results, opinions, findings, and conclusions presented in this report are those of the authors and do not necessarily reflect the views of the funding agencies.

The authors acknowledge the support of the Laboratory of Structural Engineering staff at ETH Zurich.

References

- Abbiati, G., & Stojadinovic, B. (2018). Multi-Axial Subassemblage Testing stand for hybrid simulations up to six physical Degrees-Of-Freedom. In 16th European Conference on Earthquake Engineering (16 ECEE).
- ACI Committee 318. (2014). Building code requirements for structural concrete: (ACI 318-14); and commentary (ACI 318R-14). Farmington Hills, MI: American Concrete Institute,
- Baek, J. W., Kim, S. H., Park, H. G., & Lee, B. S. (2020). Shear-Friction Strength of Low-Rise Walls with 600 MPa Reinforcing Bars. ACI Structural Journal, 117(1).
- Calvi, P. M., Bentz, E. C., & Collins, M. P. (2017). Pure mechanics crack model for shear stress transfer in cracked reinforced concrete. ACI Structural Journal, 114(2)
- Gambarova, P. G., & Karakoç, C. (1983). A new approach to the analysis of the confinement role in regularly cracked concrete elements
- Hube, M. A., María, H. S., Arroyo, O., Vargas, A., Almeida, J., & López, M. (2020). Seismic performance of squat thin reinforced concrete walls for low-rise constructions. Earthquake Spectra, 36(3), 1074-1095.
- Li, B. (1989). Contact density model for stress transfer across cracks in concrete. Journal of the Faculty of Engineering, the University of Tokyo, (1), 9-52
- Luna, B., Whittaker, A., & Rivera, J. (2013). Seismic behavior of low aspect ratio reinforced concrete shear walls.
- Mangalathu, S., Jang, H., Hwang, S. H., & Jeon, J. S. (2020). Data-driven machine-learning-based seismic failure mode identification of reinforced concrete shear walls. Engineering Structures, 208, 110331
- Moehle, J. (2015). Seismic design of reinforced concrete buildings. McGraw-Hill Education.
- Nagae, T., Ghannoum, W. M., Kwon, J., Tahara, K., Fukuyama, K., Matsumori,T., Shiohara, H., Kabeyasawa, T., Kono, S., Nishiyama, M., Sause, R., Wallace,J. W., and Moehle, J. P. (2015). Design implications of large-scale shake table test on four-story reinforced concrete building. ACI Structural Journal,112(2):135-146.
- Terzioglu, T., Orakcal, K., & Massone, L. M. (2018). Cyclic lateral load behavior of squat reinforced concrete walls. Engineering Structures, 160, 147-160.
- Trost, B., Schuler, H. and Stojadinovic, B., 2019. Sliding in compression zones of reinforced concrete shear walls: Behavior and modeling. ACI Structural Journal, 116(5).
- Walraven, J. C. and Reinhardt, H. W. (1981). Theory and experiments on the mechanical behavior of cracks in plain and reinforced concrete subjected to shear loading. Heron, 26(1A).
- Whyte, C. A., & Stojadinovic, B. (2014). Effect of ground motion sequence on response of squat reinforced concrete shear walls. Journal of Structural Engineering, 140(8), A4014004
- Zhang, X., Zhang, S., Luo, Y., & Wang, L. (2020). Effects of Interface Orientations on Bond Strength between Old Conventional Concrete and New Self-Consolidating Concrete. ACI Structural Journal, 117(5).